Available online at www.sciencedirect.com
ScienceDirect
Journal of Colloid and Interface Science 308 (2007) 53–70
JOURNAL OF Colloid and Interface Science
www.elsevier.com/locate/jcis

# Phosphate adsorption onto hematite: An in situ ATR-FTIR investigation of the effects of pH and loading level on the mode of phosphate surface complexation

Evert J. Elzinga [a,*], Donald L. Sparks [b]

[a] *Institute of Biogeochemistry and Pollutant Dynamics, Swiss Federal Institute of Technology (ETH) Zürich, CH-8092 Zürich, Switzerland*
[b] *Department of Plant and Soil Sciences, University of Delaware, Newark, DE 19717-1303, USA*

Received 9 October 2006; accepted 21 December 2006

Available online 28 December 2006

**Abstract**

Phosphate adsorption on hematite was characterized as a function of pH (3.5–8.9) and phosphate concentration (5–500 μM) by in situ ATR-FTIR spectroscopy. Under most conditions a mixture of different (inner-sphere) phosphate complexes existed at the hematite surface, with the relative importance of these complexes varying with pH and surface coverage. Experiments using $D_2O$ and $H_2O$ indicated the presence of two protonated phosphate surface complexes at pH/pD = 3.5–7.0. Comparison to spectra of protonated aqueous phosphate species suggested that these surface complexes are monoprotonated. The difference in the IR spectra of these complexes is tentatively interpreted to result from a different surface coordination, with one surface complex coordinated in a monodentate binuclear (bridging) fashion, and the second as a monodentate mononuclear complex. Alternatively, the bridging complex may be a (protonated) monodentate mononuclear complex exhibiting strong hydrogen bonding to an adjacent surface site, and the second species a monodentate complex exhibiting limited hydrogen bonding. Formation of the bridging complex is favored at lower pH values and higher surface loadings in the 3.5–7.0 pH range. At the highest pH values studied (8.5–9.0) a third complex, interpreted to be a nonprotonated monodentate mononuclear complex, is present along with the monodentate monoprotonated surface species. The importance of the nonprotonated monodentate complex increases with increasing surface coverage at these high pH values.


*Keywords:* Adsorption; ATR-FTIR spectroscopy; Phosphate; Hematite; In situ; Speciation; Protonation; Surface complexation

## 1. Introduction

Over-application of phosphorus-containing fertilizers has lead to significant water eutrophication problems that pose a threat to human and ecological health. To evaluate the transport behavior of phosphate in aquatic and terrestrial environments, a detailed understanding of the interactions of phosphate with common mineral phases found in soils and sediments is required, since such sorption reactions control to a large extent the distribution and mobility of contaminants in natural systems.

Much research has been done on the uptake of phosphate by Fe(III)-hydroxide minerals such as goethite and ferrihydrite. Spectroscopic studies on these systems have shown that phosphate forms inner-sphere complexes at the solid–liquid interface of these substrates, and have revealed that the mechanism of phosphate complexation may vary with pH and surface coverage [1–7]. However, interpretations of the coordination of the phosphate oxyanions to the Fe(III)-oxide surface and the protonation state of the adsorption complexes have differed. The spectroscopic method most commonly used to probe phosphate surface complexes at these mineral phases is infrared (IR) spectroscopy, which is very sensitive to the coordination environment and protonation state of phosphate complexes, and therefore a useful tool for characterizing phosphate surface species at the molecular scale.

The sensitivity of IR spectroscopy toward the protonation of phosphate is well illustrated by the differences between the IR spectra of $PO_4^{3-}$(aq), $HPO_4^{2-}$(aq), $H_2PO_4^{-}$(aq), and $H_3PO_4^{0}$(aq) shown in Fig. 1. The spectra of these aqueous phosphate species

* Corresponding author.
*E-mail address:* evert.elzinga@env.ethz.ch (E.J. Elzinga).

0021-9797/$ – see front matter 
doi:10.1016/j.jcis.2006.12.061

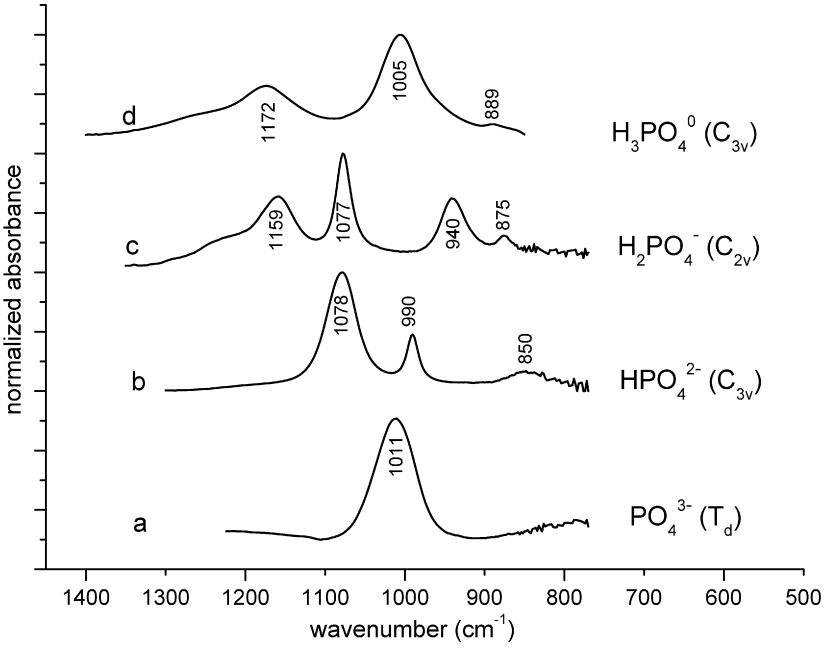


Fig. 1. ATR-FTIR spectra of aqueous $H_xPO_4^{3-x}$ phosphate species; the symmetry of the complexes is indicated in brackets. Solution pH values were as described in Tejedor-Tejedor and Anderson [5].

have also been reported by Tejedor-Tejedor and Anderson [5], and are useful for demonstrating the use of symmetry arguments in interpreting IR spectra, as outlined in Nakamoto [8]. The use of attenuated total reflectance Fourier-transform infrared (ATR-FTIR) spectroscopy in aqueous media allows for characterization of two phosphate vibrations: the nondegenerate symmetric stretching $\nu_1$, and the triply degenerate symmetric stretching $\nu_3$. The nonprotonated $PO_4^{3-}$ anion has tetrahedral symmetry and belongs to the point group $T_d$. This species has one active $\nu_3$ band, centered at 1011 $cm^{-1}$, whereas the $\nu_1$ vibration is inactive (spectrum a, Fig. 1). Protonation of this complex to $HPO_4^{2-}(aq)$ leads to a symmetry reduction from $T_d$ to $C_{3\nu}$, and as a result, the triply degenerate $\nu_3$ vibration splits into two separate $\nu_3$ bands located at 1078 and 990 $cm^{-1}$, and the $\nu_1$ band is activated and can be seen at 850 $cm^{-1}$ (spectrum b, Fig. 1). The addition of another proton to form $H_2PO_4^-(aq)$ further reduces the symmetry to $C_{2\nu}$. This symmetry reduction leads to splitting of the $\nu_3$ vibration into three $\nu_3$ bands at 1159, 1077 and 940 $cm^{-1}$, and the $\nu_1$ band remains active (at 875 $cm^{-1}$), so that a total of four bands are present for this phosphate species (spectrum c, Fig. 1). Formation of $H_3PO_4^0(aq)$ increases the symmetry back up to $C_{3\nu}$, and as a result, two $\nu_3$ bands (at 1172 and 1005 $cm^{-1}$) and one $\nu_1$ band (at 889 $cm^{-1}$) are seen for this phosphate complex (spectrum d, Fig. 1). The spectra of the $H_2PO_4^-(aq)$ and $H_3PO_4^0(aq)$ complexes also contain a broad band at ∼1220–1240 $cm^{-1}$, which has been assigned to the $\delta$(POH) bending mode [1].

The relation between the number of IR active bands and the symmetry of the phosphate anion illustrated in Fig. 1 can be used to interpret phosphate bonding configurations at mineral surfaces. For instance, when phosphate forms a nonprotonated monodentate inner-sphere complex, the symmetry of the phosphate molecule is $C_{3\nu}$, and two $\nu_3$ bands are expected to be present in addition to the active $\nu_1$ band. When phosphate forms a monodentate binuclear (i.e., bridging) or a bidentate mononuclear (i.e., edge-sharing) inner-sphere complex, the symmetry of the surface complex is $C_{2\nu}$ so that three active $\nu_3$ bands should be present in addition to the $\nu_1$ band. Surface complexes having symmetry lower than $C_{2\nu}$ (i.e., $C_1$ complexes) also will have three active $\nu_3$ peaks and one $\nu_1$ band. If phosphate coordinates as an outer-sphere complex, slight shifting in the $\nu_3$ vibrations is expected relative to those of the phosphate ions in solution due to distortion resulting from the near-surface electrical field, but the number of $\nu_3$ bands is not expected to change.

Although IR spectroscopy is highly sensitive to coordination environments and protonation states of oxyanions such as phosphate, interpretation of IR spectra is not necessarily straightforward, and often hindered by a lack of appropriate reference compounds that can be used for fingerprinting. Additionally, differences in data acquisition conditions (most notably the use of in situ versus ex-situ data collection) may affect the results obtained, and thereby the conclusions reached. Results from ex-situ experiments (i.e., data collected under dry conditions) should be viewed with caution, as sample drying may cause structural alterations in the surface complexes, leading to results that are not representative of the surface speciation occurring under in situ conditions (i.e., with water present). Differences in data acquisition conditions may, in addition to the lack of appropriate reference compounds, at least partially explain the different interpretations made in previous studies as to the speciation of phosphate surface complexes formed on Fe(III)-(hydr)oxide surfaces. A further consideration is that differences in surface site characteristics and overall reactivity toward dissolved phos-

phate between different Fe(III)-(hydr)oxide phases may lead to differences in the types of phosphate surface complexes formed.

In this study, phosphate sorption to hematite was characterized using in situ attenuated total reflectance Fourier-transform infrared (ATR-FTIR) spectroscopy. The usefulness of this specific IR technique in characterizing sorption of oxyanions such as phosphate, sulfate, borate and carbonate to metal oxide mineral phases under in situ conditions has been demonstrated in previous studies (e.g., [9–23]). In contrast to ferrihydrite and goethite, no in situ IR studies have been reported on phosphate complexation by hematite. In the experiments described here, the effects of pH and surface coverage on the mode of phosphate uptake by hematite were characterized, and the results obtained are compared to results from previous IR studies dealing with phosphate sorption to Fe(III)-(hydr)oxide mineral phases. Experiments were performed in both $H_2O$ and $D_2O$, in order to investigate the possible association of protons with the phosphate surface complexes.

## 2. Materials and methods

### 2.1. Hematite preparation

High surface area hematite ($\alpha$-$Fe_2O_3$) was synthesized following the method of Schwertmann and Cornell [24]. A 500 mL solution of 0.2 M ferric nitrate was titrated to pH 8 with 1 M KOH, and the resulting ferric oxide suspension was heated to 98 °C and aged at this temperature for 7 days, during which time the precipitate transformed into hematite. After 7 days, the hematite precipitate was washed several times with deionized water by centrifugation and decantation until the nitrate concentration was reduced to <0.003 mM. The hematite paste was then freeze-dried. The surface area of the hematite solid as determined by the five-point $N_2$–Brunauer–Emmett–Teller (BET) method was 56 $m^2\,g^{-1}$.

### 2.2. ATR-FTIR experiments

#### 2.2.1. Flow cell experiments: pH envelope and adsorption isotherms

The ATR-FTIR spectra of phosphate–hematite surface complexes were collected on a Perkin–Elmer 1720× spectrometer equipped with a purge gas generator and a liquid $N_2$-cooled MCT detector. Sorption isotherms and pH envelopes were measured using the flow cell technique described by Hug and Sulzberger [10], Hug [11], and Peak et al. [12,17]. For these experiments, a 45° ZnSe ATR crystal was coated with ≈2.5 mg of dispersed hematite and then placed inside the flow cell. The flow cell was placed on the horizontal ATR sample stage inside the IR spectrometer and connected to an $N_2$-purged reaction vessel containing 1 L of background electrolyte solution (0.01 M NaCl in DDI–$H_2O$), which was stirred with a magnetic bar, and adjusted to the desired pH. A peristaltic pump was used to pass solute from the reaction vessel through the flow cell at a known flow rate. The flow cell effluent was collected as waste, and the pH of the solution in the main reaction vessel was continuously monitored, and (re)adjusted as necessary. The experimental flow-cell setup and the technique used for depositing the hematite solid onto the ZnSe crystal are described in more detail in Peak et al. [12] and Wijnja and Schulthess [15].

Experiments were started by pumping the background electrolyte through the flow cell at a flow rate of ≈1 mL $min^{-1}$, and allowing the hematite deposit to equilibrate with the background solution. Background spectra, consisting of the absorbances of the ZnSe crystal, the hematite deposit and the electrolyte solution, were collected regularly during this equilibration period; typically after about 3 h, successive background spectra showed no further changes, indicating that the hematite deposit had equilibrated with the background solute. The final background spectrum was collected at this time as the average of 4000 scans at a 4 $cm^{-1}$ resolution, and phosphate was injected into the reaction vessel to start the adsorption experiment. All successive spectra were ratioed to this background spectrum.

For the pH envelope experiment, the initial 0.01 M NaCl background solution pumped through the flow cell had been adjusted to pH 8.6. Following equilibration of the hematite deposit with this solution and collection of the background spectrum, phosphate was added at a concentration of 25 μM. Phosphate adsorption on the hematite deposit was monitored by collecting IR spectra every 15 min. When there were no differences between successive spectra, the final spectrum of sorbed phosphate was collected as the average of 4000 scans, and the pH of the solution in the reaction vessel was lowered to pH 7.5 by addition of 0.1 M HCl. Phosphate adsorption to the hematite deposit in the flow cell was allowed to reach a new equilibrium, then the final IR spectrum was collected and pH was lowered to the next level. This procedure was repeated down to pH 3.5, in pH decrements of 0.5–1 pH units.

The phosphate adsorption isotherm measurements were performed at fixed pH values of 9.0 and 4.5. For these experiments, the hematite deposit was first equilibrated with the 0.01 M NaCl background electrolyte adjusted to the pH of interest, and next phosphate was injected at a concentration of 5 μM. Phosphate adsorption onto the hematite coating inside the flow cell was allowed to reach equilibrium; then, the final IR spectrum of sorbed phosphate was collected, and the phosphate concentration in the reaction vessel was raised for new equilibration. This procedure was repeated until the aqueous phosphate concentrations in the main reaction vessel reached 500 μM. Preliminary experiments using noncoated ZnSe crystal indicated that contributions from aqueous phosphate in the IR spectrum become visible above noise level at solution concentrations of approximately 700 μM. The ATR-FTIR spectra collected in the pH envelope and phosphate isotherm experiments are therefore dominated by absorbances from hematite-sorbed phosphate complexes, and contributions from aqueous phosphate are negligible.

#### 2.2.2. Trough experiments

In addition to the flow-cell experiments, a number of trough experiments were performed as well. Both $H_2O$ and $D_2O$ were used in these experiments, in order to investigate the involvement of protons in phosphate surface complexation by

hematite. For these measurements, a 45° ZnSe crystal coated with hematite was placed in an IR trough capable of holding 10 mL of solution. The trough was placed on the ATR sample stage inside the spectrometer, and an 8 mL volume of background electrolyte (0.01 M NaCl in either $H_2O$ or $D_2O$) adjusted to the pH/pD of interest was added. The trough was then sealed, and the hematite deposit was allowed to equilibrate with the background electrolyte. Once a stable background was obtained, phosphate was added to the solution at the appropriate concentration. Following equilibration, the final IR spectrum was collected, and 1.5 mL of solute was withdrawn from the trough and measured for pH/pD. Next, either the pH/pD of the solution remaining in the trough was lowered by addition of 0.1 M HCl or DCl, or the phosphate concentration of this solution was raised, depending on the experiment. A new equilibrium was allowed to get established, the final spectrum was collected, and the trough solution was measured for pH/pD. Following the adsorption experiments, all solutes used in these experiments were scanned (using noncoated ZnSe ATR crystals) to ensure that contributions from aqueous phosphate species were negligible in the IR spectra of the sorption experiments.

#### 2.2.3. Spectral peak fitting

The Peaksolve software package version 1.05 (Galactic Industries Corp.) was used for peak deconvolution and to determine the number and symmetry of phosphate surface complexes present. A linear baseline was fitted between 1200 and 880 $cm^{-1}$ in the raw spectra, and the spectra were normalized to the highest peak intensity. These normalized, baseline-corrected spectra were fitted with Gaussian peaks. We collected a large spectral data set, which showed systematic changes in spectral band positions and intensities as reaction conditions were varied; the number of Gaussians fitted to a given spectrum was based on these systematic changes as well as on the number of peaks visible in the spectrum. The adjustable parameters optimized for each Gaussian band during fitting were the band position, band intensity and band width. No constraints were placed on these fitting parameters in any of the fits. The band width and band position for a given Gaussian peak always converged to similar values in different spectra, whereas the peak intensities varied, reflecting variation between samples in the contribution of the associated phosphate surface complexes to the overall phosphate surface speciation. The relative intensities of Gaussian peaks belonging to a given phosphate surface complex were always similar in the various spectra where the complex was present.

## 3. Results

### 3.1. pH envelope

Fig. 2A shows the ATR-FTIR spectra of phosphate complexes forming at the hematite–water interface in the pH range 3.5–8.6 at an aqueous phosphate concentration of 25 μM. The increase in intensity of the IR absorbances with decreasing pH indicates that phosphate sorption increases when pH is lowered, which is consistent with macroscopic results showing that phosphate sorption to Fe(III)-oxide mineral phases increases with decreasing pH [5,7]. In addition to intensity changes, significant changes in spectrum shape are observed as a function of pH as well. At the two highest pH values (pH 8.6 and 7.5), the spectra are dominated by three IR frequencies, centered at approximately 1085, 1040 and 960 $cm^{-1}$. When the pH is lowered, the band at 1085 $cm^{-1}$ gradually shifts to higher wavenumbers, and additional frequencies appear at ∼1000 and 970 $cm^{-1}$ (Fig. 2A). The pH 4.8 and 5.4 spectra show evidence for the presence of at least four bands, as indicated by the presence of two peak maxima and two shoulders occurring on the low wavenumber side of the band with the lower peak maximum location. At the lowest pH value (pH 3.5), three bands are distinguishable in the 1200–900 $cm^{-1}$ wavenumber region, at spectral locations of approximately 1120, 1010, and 970 $cm^{-1}$ (Fig. 2A).

As discussed in the Introduction, the maximum number of phosphate $\nu_3$ bands expected based on symmetry arguments is three. In the spectral region shown in Fig. 2A, the $\nu_3$ bands are expected to dominate, although $\nu_1$ bands may be present at the very low end of the wavenumber range shown. Based on comparison to the spectra of aqueous phosphate complexes shown in Fig. 1, we conclude that the bands observed in Fig. 2A are the $\nu_3$ bands of sorbed phosphate species, with no evidence for the presence of active $\nu_1$ bands. The $\nu_1$ bands are probably located at wavenumbers lower than 900 $cm^{-1}$, where they are obscured by vibrational bands of water and the hematite sorbent.

The spectra collected at pH 8.6 and 7.5 are characterized by three well-defined $\nu_3$ bands, suggesting the presence of a single phosphate species at these pH values, with a $C_{2v}$ or lower symmetry. The pH 3.5 and 4.0 spectra also appear to have three $\nu_3$ bands, which could indicate the presence of a single phosphate species at these pH values as well. However, the gradual, systematic shifting of bands with pH in the pH range 7.0–3.5, combined with the apparent presence of at least four $\nu_3$ bands at pH 4.8 and 5.4 suggests that the phosphate IR spectra observed between pH 7.0 and 3.5 consist of the combined absorbances of at least two different phosphate surface complexes: the phosphate complex that dominates at high pH, and a second surface complex that grows in as the pH is lowered. To investigate this option, we took the difference spectra of the data collected at pH 8.6, 7.0, 5.4, and 3.5, in order to isolate the IR spectra of the (additional) phosphate species coordinating to the hematite surface when pH is lowered. The results are shown in Fig. 2B. The difference spectra in all cases show two strong vibrational bands at approximately 1115 and 1006 $cm^{-1}$, along with a weaker band at about 970 $cm^{-1}$ that appears as a shoulder on the 1006 $cm^{-1}$ frequency. These three $\nu_3$ bands are especially well-defined in the difference spectra of the data collected in the pH range 3.5–7.0, whereas the difference spectrum of the data collected at pHs 8.6 and 6.4 appears to contain additional frequencies corresponding to the IR spectrum of phosphate sorbed at high pH (Fig. 2B). The difference spectra shown in Fig. 2B indicate that lowering pH leads to the formation of a phosphate surface complex that has an IR spectrum very different from

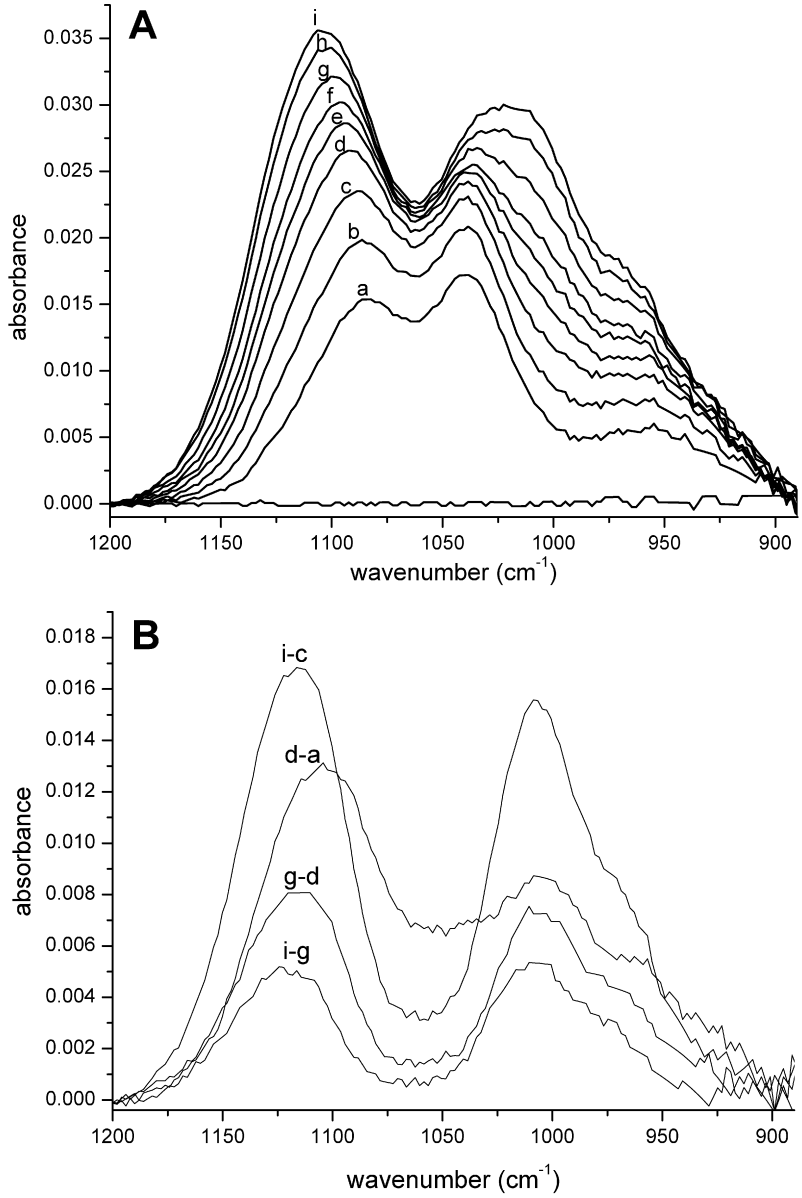


Fig. 2. (A) Results from the flow-cell pH envelope experiment, conducted at $[PO_4] = 25$ μM. The spectra were collected at pH (a) 8.6, (b) 7.5, (c) 7.0, (d) 6.4, (e) 5.9, (f) 5.4, (g) 4.8, (h) 4.0, and (i) 3.5. (B) shows the difference spectra of selected spectra from figure (A).

that of the phosphate species dominating the surface speciation at high pH.

Although not shown, the (normalized) experimental spectra observed in the pH range 3.5–7.0 could be quite successfully reproduced with linear combination fits of the (normalized) pH 8.6 spectrum and the normalized difference spectrum of the spectra collected at pH 3.5 and 7.0. We do not show these linear combination fits, since results from experiments performed in $D_2O$ (presented in a later section) suggest that the experimental spectrum collected at pH 8.6 likely contains contributions from two different phosphate surface complexes, thereby making this spectrum unsuitable to serve as an endmember representing a single phosphate surface species. These results do, however, indicate that at least two different phosphate complexes are present at the hematite surface in the pH range 3.5–7.0.

### *3.2. Adsorption isotherms*

The results from the isotherm experiment performed at pH 4.5 are shown in Fig. 3A, which presents the IR spectra of phosphate–hematite sorption complexes forming at aqueous phosphate concentrations ranging between 5 and 500 μM. The IR absorbance intensities increase with increasing phosphate concentrations, indicating that the amount of phosphate sorbed increases as the phosphate concentration is raised. This indicates that hematite surface site saturation is not achieved in the phosphate concentration range applied here.

Consistent with the results from the pH envelope experiment described in the previous section, the IR spectra of sorbed phosphate at pH 4.5 shown in Fig. 3A appear to consist of the absorbances of at least two different phosphate sorption

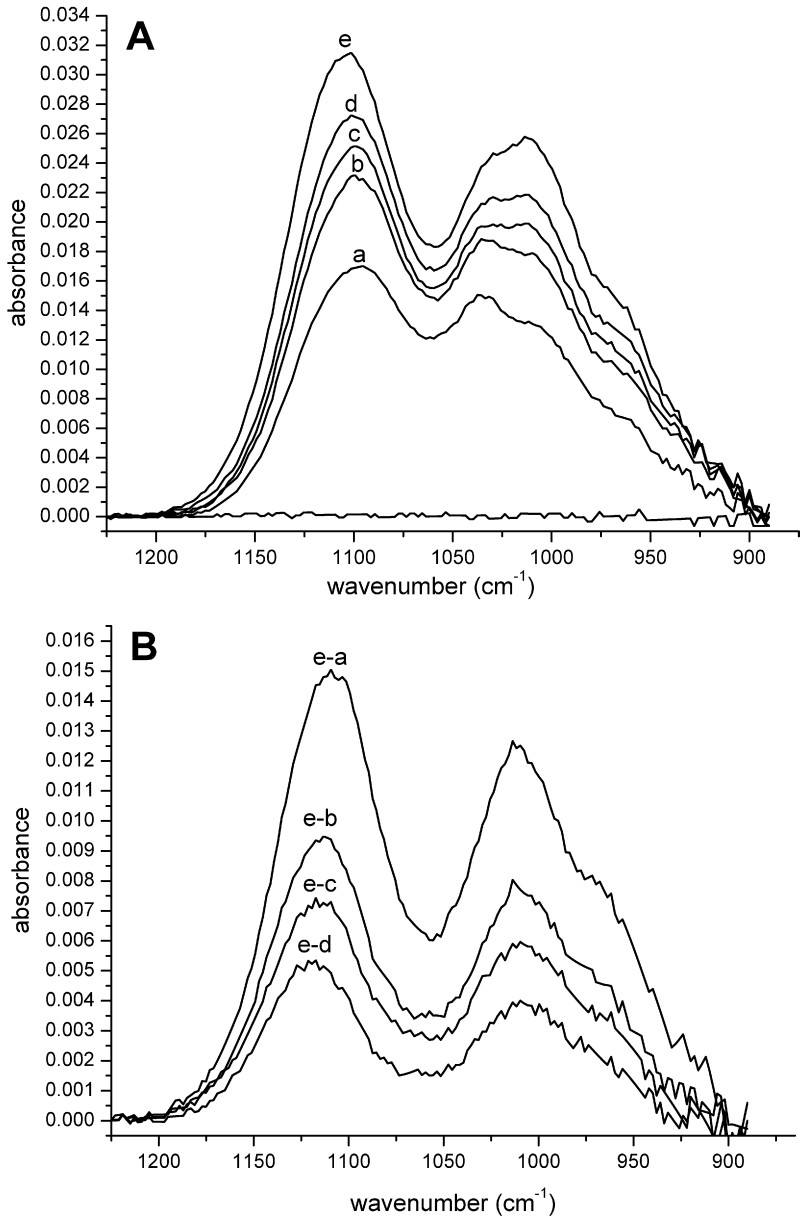


Fig. 3. (A) ATR-FTIR data of adsorbed phosphate obtained from the flow-cell adsorption isotherm experiment conducted at pH 4.5. Spectra were collected at aqueous phosphate concentrations of (a) 5 μM, (b) 10 μM, (c) 25 μM, (d) 50 μM, and (e) 500 μM. (B) shows the difference spectra of the spectrum collected at the highest phosphate concentration and those collected at the lower phosphate concentrations.

complexes. There is a change in spectrum shape, however, as the phosphate concentration increases, indicating that the phosphate surface speciation changes with surface loading. To characterize the phosphate surface species forming preferentially as the surface loading increases at pH 4.5, we took the difference spectra of the spectrum collected at the highest phosphate concentration and those of the lower phosphate concentrations. These difference spectra are shown in Fig. 3B, and in all cases show a strong resemblance to the spectrum of the phosphate species identified in the previous section as forming preferentially with decreasing pH, having strong vibrational bands at approximately 1115 and 1010 $cm^{-1}$, along with a weaker band at about 970 $cm^{-1}$ that appears as a shoulder on the 1010 $cm^{-1}$ frequency (Figs. 3B and 2B). This indicates that, when increasing the surface loading at a fixed pH value of 4.5 by increasing the solution concentration of phosphate, the phosphate surface speciation is increasingly influenced by the same phosphate species that forms preferentially when the phosphate surface loading is increased by lowering pH (at a fixed phosphate solution concentration) in the pH range 3.5–7.0.

The results of the adsorption isotherm experiment performed at pH 9.0 are presented in Fig. 4A for aqueous phosphate concentrations between 5 and 500 μM. Regardless of concentration, the ATR-FTIR spectra of sorbed phosphate at this high pH value are dominated by three $\nu_3$ bands located at approximately 1085, 1040, and 960 $cm^{-1}$, consistent with the results from the pH edge experiments described in the previous section.

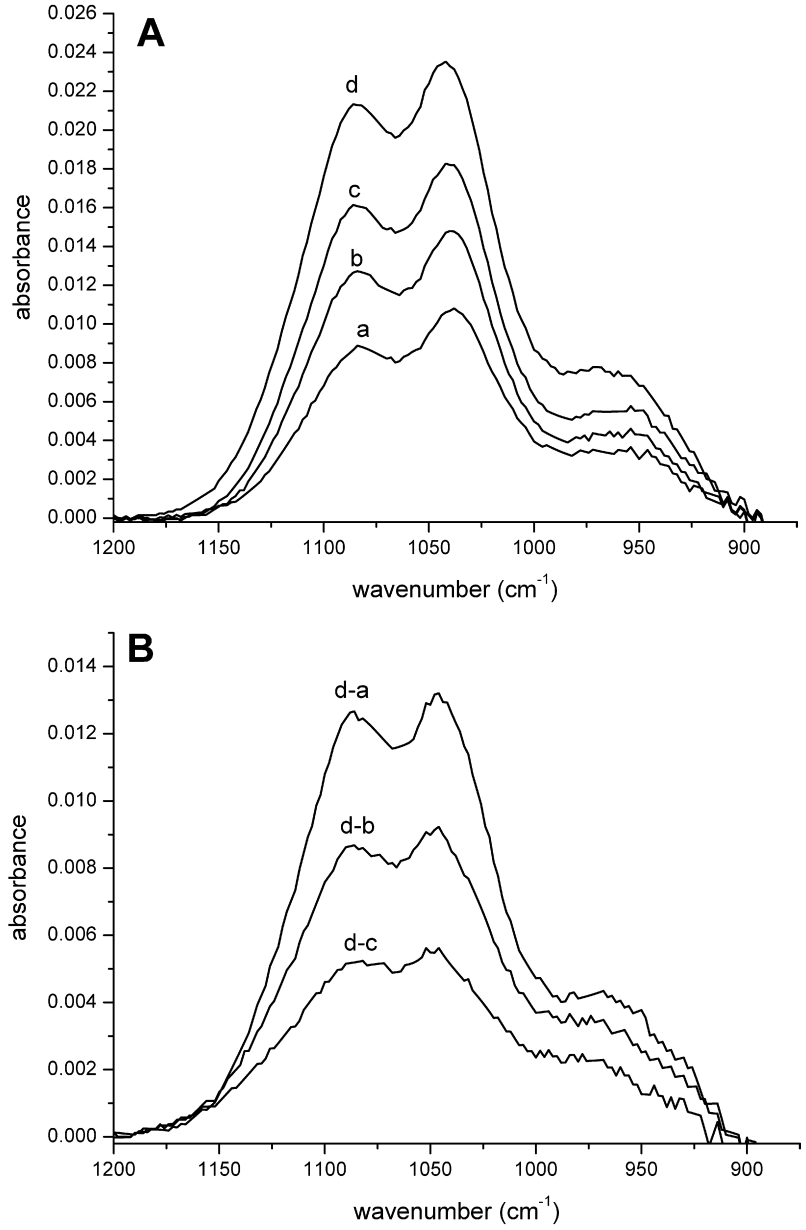


Fig. 4. (A) ATR-FTIR data of adsorbed phosphate obtained from the flow-cell adsorption isotherm experiment conducted at pH 9.0. Spectra were collected at aqueous phosphate concentrations of (a) 5 μM, (b) 25 μM, (c) 100 μM, and (d) 500 μM. (B) shows the difference spectra of the spectrum collected at 500 μM and those collected at the lower phosphate concentrations.

Although the spectra of the sorption complexes collected at the various phosphate concentrations overall look quite similar at pH 9.0, a subtle change seems to occur in the IR spectra as the phosphate concentration is raised: the relative intensities of the $\nu_3$ bands change, and there is the suggestion of an additional frequency arising at approximately 975 $cm^{-1}$ (Fig. 4A). The difference spectra between the data collected at the highest phosphate concentration and the lower phosphate concentrations are shown in Fig. 4B, and bring out these features more clearly. The change in the IR spectrum observed at higher phosphate concentrations suggests the presence of an additional phosphate surface complex that becomes increasingly pronounced at higher phosphate surface coverage. However, given the overall similarity between the difference spectra shown in Fig. 4B and the spectra collected at low phosphate concentrations, it is not likely that taking the difference spectrum has fully isolated the IR spectrum of this additional species. More likely, the difference spectra shown in Fig. 4B represent a mixture of the surface complexes forming at lower phosphate concentrations and the other species that starts forming (or becomes more pronounced) at the higher phosphate concentrations. Further evidence for the presence of multiple phosphate surface species at these high pH values, and additional information on the identity of the various species formed will be provided below.

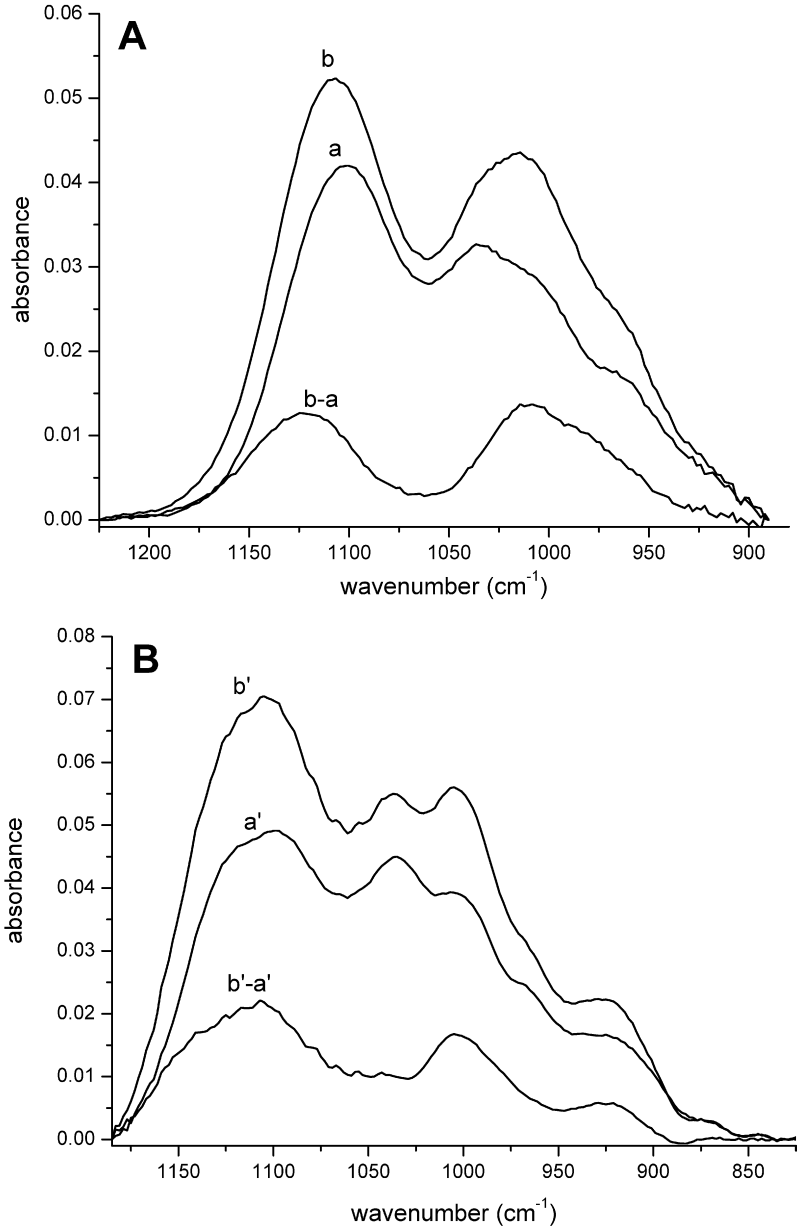


Fig. 5. Results from the trough experiments conducted in $H_2O$ and $D_2O$ at a phosphate concentration of 300 μM. (A) shows the data from the $H_2O$ experiments, with spectrum a collected at pH 6.1 and spectrum b at pH 3.6. (B) shows the data from the $D_2O$ experiment, with spectrum a′ collected at pD 6.2 and spectrum b′ at pD 5.4. (C) compares the difference spectra of the high and low pH/pD spectra from figures (A) and (B).

### *3.3. Trough experiments*

Trough experiments were conducted with the aim to compare phosphate IR spectra collected in $D_2O$ and $H_2O$ backgrounds in order to investigate the possible involvement of protons in the phosphate–hematite surface complexes. If protons take part in the coordination of phosphate to the hematite surface, the IR bands associated with the P–OH stretching vibrations in particular are expected to shift to lower wavenumbers when $D_2O$ is used instead of $H_2O$.

Fig. 5 shows the results of two experiments that were done in a similar manner, except that $H_2O$ was used in one experiment (Fig. 5A) and $D_2O$ in the other (Fig. 5B). The aim of both experiments was to isolate the spectrum of the phosphate surface species that becomes more pronounced with decreasing pH and with increasing phosphate surface loadings in the pH range 3.5–7.0 (represented by spectrum i-c in Fig. 2B, and the various difference spectra shown in Fig. 3B). The results from the pH envelope experiment described earlier indicated that this species dominates the additional phosphate sorption occurring when pH is lowered in the pH range 3.5–7.0 (Fig. 2). Based on this information, hematite was first equilibrated at near neutral pH/pD = 6.2 with a total phosphate concentration of 300 μM. Following equilibration, the spectrum of adsorbed phosphate was collected, yielding spectrum a shown in Fig. 5A ($H_2O$), and spectrum a′ in Fig. 5B ($D_2O$). Next, the pH/pD of the solution was lowered by addition of HCl or DCl (to final pH = 3.9 in the $H_2O$ experiment, and to final pD = 5.2 in

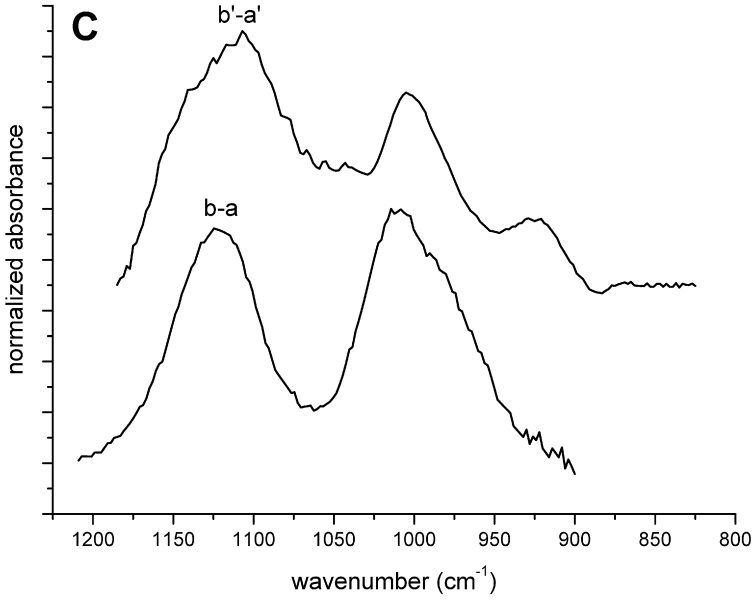


Fig. 5. (*continued*)

the $D_2O$ experiment), and a new sorption equilibrium (with a larger amount of phosphate sorbed) was allowed to get established. Although the final pD value (5.2) is different from the final pH value (3.9) in these experiments, the results shown in Fig. 2 suggest that the *additional* phosphate uptake occurring when lowering pH/pD from 6.2 to 5.2 or 3.9 occurs by the same mechanism, and leads to the preferred formation of the (single) phosphate species represented by the i-c difference spectrum shown in Fig. 2B, which we attempt to further characterize here. The phosphate IR spectra collected under these new equilibrium conditions (with lower pH/pD) are presented in Fig. 5 as spectrum b (Fig. 5A) and spectrum b′ (Fig. 5B) for the $H_2O$ and $D_2O$ experiments, respectively. The difference spectrum between the two IR scans thus obtained isolated the phosphate surface species of interest, as illustrated in Fig. 5A, which presents the results of the $H_2O$ experiment. As can be seen, the difference spectrum of the two IR spectra obtained in this experiment is very similar to the spectrum i-c in Fig. 2B as well as the spectra shown in Fig. 3B, indicating successful isolation of the IR spectrum of the target phosphate surface species. The two IR spectra collected in the $D_2O$ experiment (performed in the same way as the $H_2O$ experiment) are shown in Fig. 5B, along with the difference spectrum of these two spectra, which represents the IR spectrum of the target phosphate surface complex in $D_2O$. The non-Gaussian shape of the IR peak located at 1120 $cm^{-1}$ in the $D_2O$ difference spectrum is due to the presence of the intense D–O–D bending vibration at 1230 $cm^{-1}$, which complicated background removal in this region.

Fig. 5C compares the (normalized) difference spectra obtained in the $H_2O$ and $D_2O$ experiments, characterizing the phosphate surface complex that forms preferentially with decreasing pH and increasing surface loading in the pH/pD range 3.5–7.0. The comparison clearly shows that band shifting toward lower wavenumbers occurs when switching from $H_2O$ to $D_2O$. Although all three $\nu_3$ bands seem to move to some extent toward lower frequencies when using $D_2O$, a particularly large shift is observed for the $\nu_3$ band located at the lowest wavenumber, which shifts from ∼975 $cm^{-1}$ in water to ∼925 $cm^{-1}$ in $D_2O$ (Fig. 5C). Overall, the results presented in Fig. 5 indicate that the phosphate surface complex that becomes increasingly important with decreasing pH and with increasing phosphate surface loadings at pH 3.5–7.0 is a protonated phosphate adsorption complex.

A second set of experiments similar to those described above were performed at pH/pD values >8, in order to investigate the possible protonation of the phosphate surface complexes formed at high pH/pD. Instead of changing pH/pD following initial equilibration as done in the $H_2O/D_2O$ experiment described above, for these high pH/pD experiments the phosphate concentration was raised following initial equilibration at a relatively low concentration. This was done based on the results from the pH 9.0 adsorption isotherm experiment described in Section 3.2, which indicated a possible surface speciation change with increasing phosphate solution concentration. The results from both experiments are shown in Fig. 6. In Fig. 6A, the results from the $H_2O$ experiment are presented, with spectrum a collected at a phosphate concentration of 75 μM (final pH = 8.0), and spectrum b at a phosphate concentration of 300 μM (final pH = 8.2). Similar to the pH 9.0 isotherm data shown in Fig. 4, increasing the phosphate concentration leads to a change in the relative intensities of the $\nu_3$ bands located at 1085 and 1040 $cm^{-1}$, and the appearance of an additional frequency at approximately 975 $cm^{-1}$. The difference spectrum for the spectra collected at high and low phosphate concentration emphasizes this change (Fig. 6A), and is consistent with the difference spectrum found in the pH 9.0 adsorption isotherm shown in Fig. 4.

The results from the $D_2O$ experiment performed at high pD are shown in Fig. 6B, with spectrum a′ collected at a phosphate concentration of 25 μM (final pD = 8.1), and spectrum b′ at a phosphate concentration of 100 μM (final pD = 8.7). Three im-

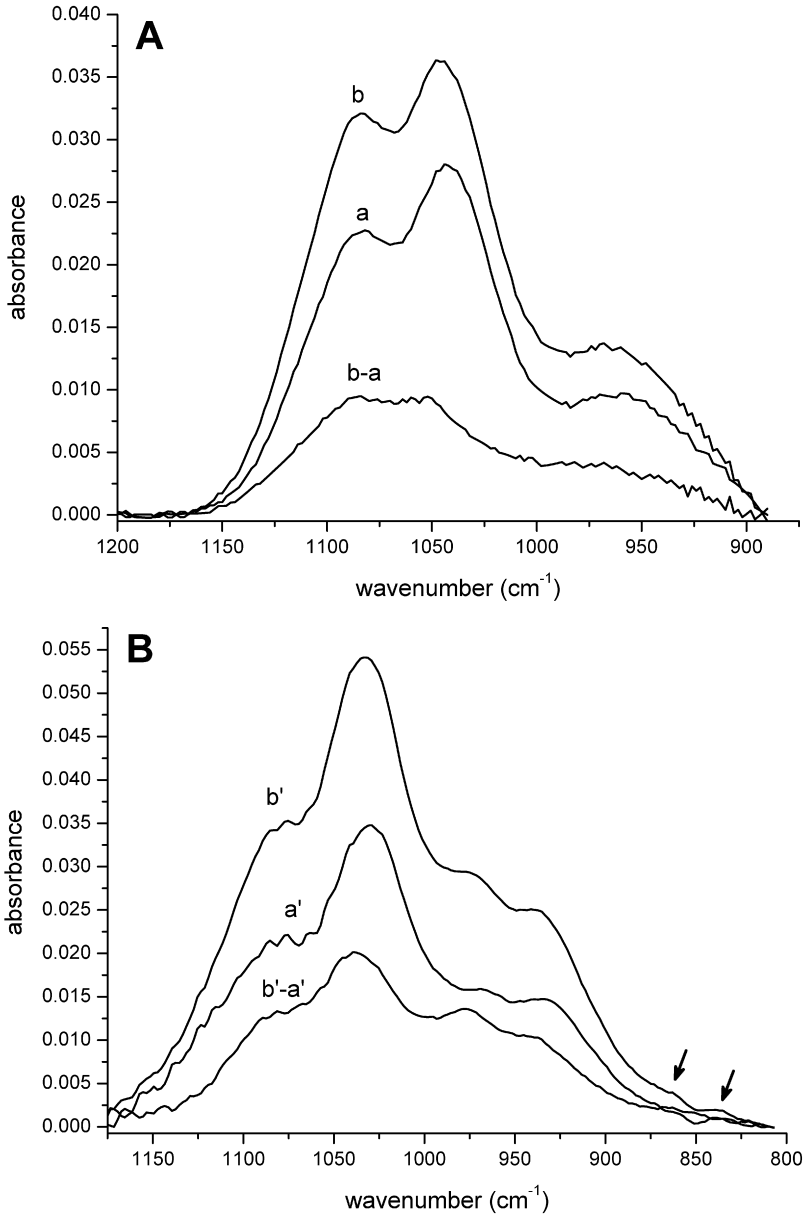


Fig. 6. Results from the trough experiments conducted in $H_2O$ and $D_2O$ at pH/pD > 8. (A) shows the data from the $H_2O$ experiments, with spectrum a collected at $[PO_4] = 75$ μM and pH 8.0, and spectrum b at $[PO_4] = 300$ μM and pH 8.2. (B) shows the data from the $D_2O$ experiment, with spectrum a′ collected at $[PO_4] = 25$ μM and pD 8.1, and spectrum b′ at $[PO_4] = 100$ μM and pD 8.7. The arrows indicate $\nu_1$ bands visible in spectrum b′. (C) compares selected spectra from figures (A) and (B).

portant observations can be made from these $D_2O$ data. Firstly, compared to the spectra obtained in water (Fig. 6A), some $\nu_3$ bands have shifted to lower wave numbers, indicating the presence of protonated phosphate surface complexes at these high pD values. Secondly, four $\nu_3$ bands are discernible in the $D_2O$ IR spectra shown in Fig. 6B, as opposed to three in the $H_2O$ data. Thirdly, there appear to be two $\nu_1$ bands present in the $D_2O$ spectra, at band positions of approximately 870 and 840 $cm^{-1}$, as indicated by the arrows in Fig. 6B. Combined, these observations confirm the presence of two different phosphate complexes at the hematite surface at high pH/pD, as alluded to in the results of the $H_2O$ experiments, and the observed band shifting to lower wavenumbers in $D_2O$ as compared to $H_2O$ indicates that at least one of these complexes is protonated. The two complexes have strongly overlapping $\nu_3$ bands, which makes their individual distinction difficult, especially when using $H_2O$. Working in $D_2O$, however, leads to band shifting for at least one of the phosphate complexes, as a result of which $\nu_3$ band separation occurs that allows for individual $\nu_3$ bands to be identified more clearly.

In Fig. 6C, the (normalized) difference spectra collected in $D_2O$ and $H_2O$ are compared, and also shown are the high concentration samples collected in $D_2O$ and $H_2O$. Obviously, there are significant differences between the difference spectra collected in $H_2O$ and $D_2O$, consistent with the presence of protonated phosphate species in these samples as noted before. The

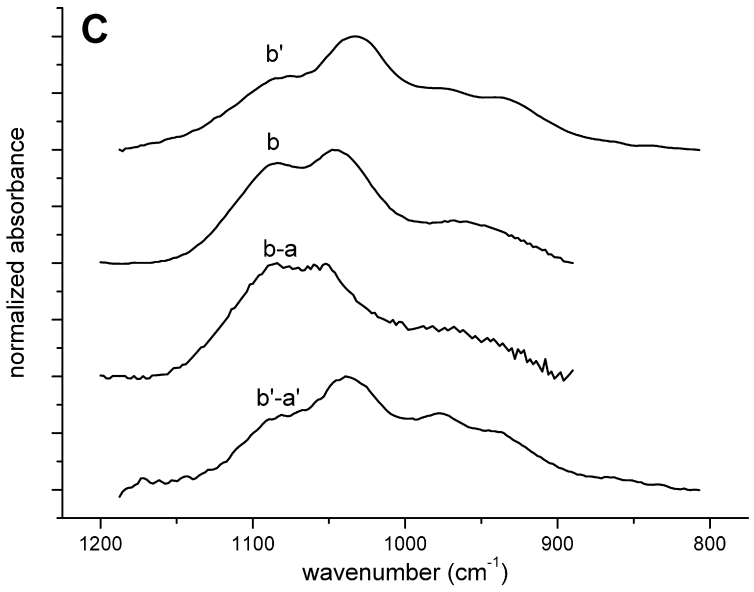


Fig. 6. (*continued*)

two difference spectra are, however, not necessarily very different from the respective sets of original spectra they were derived from. This suggests that these difference spectra do not represent an individual phosphate surface complex, but probably still contain contributions from both phosphate species present at these high pH/pD values. Therefore, we were not successful in isolating the IR spectrum of the additional phosphate complex that becomes increasingly important as the phosphate concentration is raised in the high pH/pD range. Results from spectral data fitting for further characterization of the two phosphate species formed at these high pH/pD values are described below.

### 3.4. Spectral peak fitting results

For further characterization of the symmetry and identity of the various phosphate surface complexes observed, peak fitting of the IR spectra was performed. The results are shown in Figs. 7 and 8, with Fig. 7 showing the fit results for the $H_2O$ samples, and Fig. 8 those of the $D_2O$ samples. The spectrum of the phosphate complex favored under conditions of low pH and high phosphate surface loadings in the pH range 3.5–7.0 (spectrum a in Fig. 7, which is the same as spectrum i-c in Fig. 2B) is well reproduced with three Gaussian $\nu_3$ peaks, centered at 1117, 1007 and 964 $cm^{-1}$, confirming the $C_{2v}$ or lower symmetry of this surface species.

Spectra collected at high pH values could also be fitted with three $\nu_3$ bands, as illustrated in Fig. 7 for the spectra collected in the isotherm experiment conducted at pH 9.0, which was discussed in the previous section. The fitting results were different for low and high phosphate concentration samples however. The experimental IR spectrum of the low concentration (5 μM) sample was reasonably well reproduced using three Gaussian peaks located at approximately 1086, 1034 and 966 $cm^{-1}$ (spectrum b in Fig. 7). For the spectrum collected at a phosphate concentration of 500 μM, the fitted Gaussian peaks are centered at similar spectral location as for the low concentration sample, but there is a notable decrease in the relative intensity of the peak centered at 1035 $cm^{-1}$ (spectrum c in Fig. 7). The fit of the difference spectrum of the high and low phosphate concentration samples brings out this difference between the 500 and 5 μM spectra quite clearly (spectrum d in Fig. 7).

The $D_2O$ spectrum of the phosphate surface complex that forms preferentially with decreasing pH/pD and increasing surface loadings in the pH/pD range 3.5–7 was fitted with three Gaussian $\nu_3$ bands located at 1112, 1002, and 925 $cm^{-1}$ (Fig. 8, spectrum a). These bands are located at lower wavenumbers as compared to the spectrum of this phosphate species collected in $H_2O$ (spectrum a, Fig. 7), confirming that this surface complex is protonated. The large shift of the third $\nu_3$ band (from 964 $cm^{-1}$ in $H_2O$ to 925 $cm^{-1}$ in $D_2O$) suggests that this is the P–OH/D asymmetric stretching band.

Fitting of the spectra collected at high pD (8.3 and 8.7) required four $\nu_3$ bands. Two $\nu_1$ bands, positioned at 865 and 837 $cm^{-1}$, were also fitted for the spectrum collected at a phosphate concentration of 100 μM (spectrum c in Fig. 8); in the (lower quality) spectrum collected at a concentration of 25 μM phosphate no $\nu_1$ bands were visible above noise level (Fig. 8, spectrum b). The presence of two $\nu_1$ bands indicates that two different phosphate species are present in these high pD samples. The $\nu_3$ band with the highest frequency in these $D_2O$ samples is located at ∼1075 $cm^{-1}$, which is approximately 10 $cm^{-1}$ lower than the spectral location of this band in the $H_2O$ samples prepared at equivalent pH values (Figs. 7 and 8). The other three $\nu_3$ bands present in the $D_2O$ spectra are fitted at ∼1030, 990 and 936 $cm^{-1}$ (Fig. 8). Raising the phosphate concentration leads to an increase in the relative intensity of the band at ∼990 $cm^{-1}$, and a decrease in the intensities of the bands positioned at 1030 and 936 $cm^{-1}$, whereas the relative intensity of the band located at ∼1075 $cm^{-1}$ remains mostly

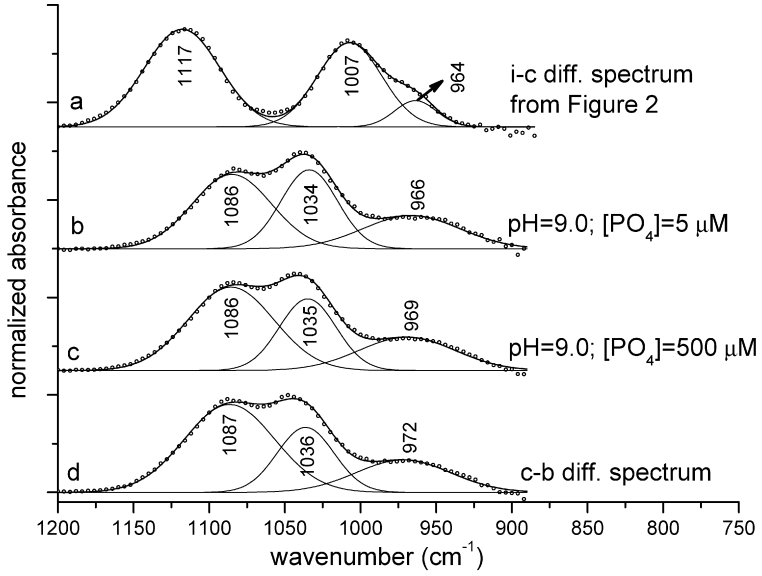


Fig. 7. Spectral deconvolution results for spectra collected in $H_2O$. Spectrum a was obtained from the pH edge results, and represents the phosphate species forming preferentially at low pH values and high surface loadings in the pH range 3.5–7.0. Spectra b, c and d were collected at pH 9.0. Raw data are indicated by the open circles, the overall fits by the black lines, and the Gaussian contributions by the gray lines.

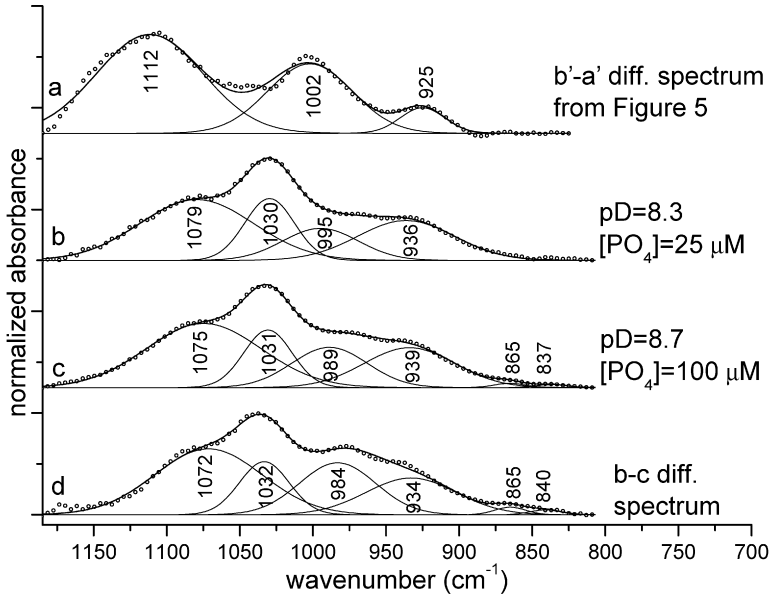


Fig. 8. Spectral deconvolution of spectra collected in $D_2O$. Spectrum a was taken from Fig. 4, and represents the phosphate species forming preferentially at low pD values and high surface loadings in the pH/pD range 3.5–7.0. Spectra b, c and d were collected at pD ∼ 8.5. Raw data are indicated by the open circles, the overall fits by the black lines, and the Gaussian contributions by the gray lines.

unchanged when the phosphate concentration is raised (spectra b and c, Fig. 8); these spectral changes are readily visible in the difference spectrum of the high and low loading samples (spectrum d, Fig. 8).

The spectral fitting results from the high pD samples are consistent with the presence of two phosphate surface species at pH/pD > 8: one with $C_{3v}$ symmetry (two $\nu_3$ bands) and the other having $C_{2v}$ or lower symmetry (three $\nu_3$ bands). The $\nu_3$ band fitted at ∼1075 $cm^{-1}$ is "shared" by these two different surface species (or contains two strongly overlapping individual $\nu_3$ bands), and therefore does not significantly change in relative intensity when the phosphate concentration is raised. The bands located at ∼1030 and 936 $cm^{-1}$ belong to the surface species with $C_{2v}$ or lower symmetry, and the relative importance of this species decreases as the surface loading increases. The $\nu_3$ band at ∼990 $cm^{-1}$ is associated with the $C_{3v}$ surface species, which grows in as the phosphate surface loading is raised. In $H_2O$, the $\nu_3$ bands of these two phosphate species strongly overlap. The broad band centered near 970 $cm^{-1}$ in the high loading $H_2O$ samples consists of two $\nu_3$ bands, which separate when using $D_2O$, so that contributions from individual peaks become visible at ∼990 and 935 $cm^{-1}$. Overlap of $\nu_3$

bands from these two species likely also occurs between 1150 and 1000 $cm^{-1}$ when working in $H_2O$. Switching to $D_2O$ leads to some shifting of individual bands in this spectral region, which changes the relative intensities of the $\nu_3$ bands present as compared to the $H_2O$ samples, but no clear separation of the bands occurs.

Band shifting to lower wavenumbers occurs for $\nu_3$ bands associated with the phosphate surface complex of $C_{2\nu}$ or lower symmetry (which dominates the surface speciation at low surface loadings in the high pH/pD samples) when switching from $H_2O$ to $D_2O$, indicating that this phosphate species is protonated. This band shifting is most apparent from the appearance of the $\nu_3$ band at 935 $cm^{-1}$ as a separate band in $D_2O$.

The complex having $C_{3\nu}$ symmetry (which grows at higher surface loadings at high pH) has not been fully isolated in the $H_2O$ experiments due to the noted strong overlap with the bands from the other complex, and this complicates the comparison of the $H_2O$ and $D_2O$ IR spectra of this species. The $\nu_3$ band fitted at 1087 $cm^{-1}$ in the $H_2O$ samples shifts slightly to 1075 $cm^{-1}$ in the $D_2O$ samples; however, this band is shared with the other surface complex present at high pH/pD, which is protonated, and may therefore be mostly responsible for this shift. The other $\nu_3$ band associated with the $C_{3\nu}$ phosphate species, fitted at 984–995 $cm^{-1}$ in the $D_2O$ data, is not seen as an individual band in the $H_2O$ samples, and therefore no direct comparison can be made with the position of this band in $H_2O$, although it can be concluded that if any shift occurs at all for this band, it would be small. Due to the spectral overlap with the $C_{2\nu}$ surface complex, the protonation state of the $C_{3\nu}$ phosphate surface species cannot be resolved based on our ATR-FTIR data; further considerations on the identity and protonation state of this surface complex will be discussed in Section 4.2.

The strong spectral overlap of the $C_{3\nu}$ and $C_{2\nu}$ species present at the hematite surface at high pH in the $H_2O$ experiments makes it difficult to determine the contribution of each species in a given spectrum. The fit results from the low concentration (25 μM) $D_2O$ experiment conducted at pD 8.5 indicate a substantial contribution from the $C_{3\nu}$ complex even at this low concentration. This suggests that most (if not all) high pH (8.0–9.0) spectra reported here contain contributions from both the $C_{3\nu}$ and $C_{2\nu}$ species, with the importance of the $C_{3\nu}$ contribution increasing with increasing phosphate concentrations.

## 4. Discussion

### 4.1. Comparison to previous studies

There have been a number of previous studies dealing with ATR-FTIR characterization of phosphate complexes forming on Fe(III)-(hydr)oxide mineral surfaces, including goethite [5,6], ferrihydrite [7], and hematite [6]. Due to differences in IR data acquisition techniques (most notably the use of in situ versus ex-situ conditions during data collection), differences in reaction conditions (e.g., phosphate:substrate ratios, substrate pretreatment) and differences between the various Fe(III)-(hydr)oxide minerals studied with respect to surface site characteristics and overall reactivity toward dissolved phosphate, the results from these previous studies are not necessarily directly comparable to those presented here for phosphate complexation by hematite. Nevertheless, in a broad sense, similarities in phosphate complexation mechanisms on these various Fe(III) substrates can be identified.

Tejedor-Tejedor and Anderson [5] studied phosphate surface complexes forming on goethite, using in situ IR spectroscopy to characterize the phosphate surface speciation as a function of pH (3.6–8.0) and phosphate surface loading (100–190 μmol $g^{-1}$). Similar to our findings, three different phosphate complexes were identified, and the relative importance of these complexes varied with pH and surface coverage. In the low to intermediate pH range (3.6–6.5), decreasing pH and increasing the phosphate loading favored the formation of a surface complex with IR bands located at approximately 1123, 1006 and 982 $cm^{-1}$, whereas higher pH values and lower phosphate surface coverages in this pH range favored the formation of a phosphate complex with IR bands at 1096 and 1044 $cm^{-1}$. The first complex is quite similar to the phosphate complex that preferentially forms on hematite at low pH and high surface coverage in the pH range 3.5–7.5, with IR bands positioned at 1117, 1007 and 964 $cm^{-1}$ (Figs. 2 and 8). Tejedor-Tejedor and Anderson [5] assigned this species as a bridging (i.e., monodentate binuclear) monoprotonated phosphate complex, based mostly on the position of the P=O band at 1125 $cm^{-1}$.

The two IR bands of the second complex observed by Tejedor-Tejedor and Anderson [5], favored at high pH and low surface coverage in the 3.5–6.5 pH range, are quite similar to the higher frequency bands we observe for the phosphate complexes forming on hematite at high pH and low surface coverage, having IR bands at 1086, 1034 and 966 $cm^{-1}$ (Figs. 2 and 8). The absence of the 966 $cm^{-1}$ $\nu_3$ band in the data of Tejedor-Tejedor and Anderson [5] may indicate the formation of different surface complexes on goethite and hematite under these conditions. However, the similarity in position and relative intensity of the other two $\nu_3$ bands in our studies and those of Tejedor-Tejedor and Anderson [5] is remarkable and suggests that similar complexes may be formed on both substrates. The 966 $cm^{-1}$ band may be hard to identify in phosphate–goethite systems, due to its relatively low intensity, its proximity to a strong goethite IR band at approximately 900 $cm^{-1}$, and its overlap with $\nu_3$ bands of the other two phosphate complexes formed on goethite, which co-exist with this second species under most experimental conditions. A very recent ATR-FTIR study by Luengo et al. [25] confirms the presence of phosphate surface complexes at the goethite surface at pH > 7.5 with $\nu_3$ IR bands centered at 945, 1044, and 1089 $cm^{-1}$, similar to what is observed here for the phosphate complexes on hematite at high pH. This phosphate complex was assigned by Tejedor-Tejedor and Anderson [5] as well by Luengo et al. [25] as a bridging nonprotonated surface complex.

The third phosphate complex identified by Tejedor-Tejedor and Anderson [5] has $\nu_3$ bands located at 1025 and 1001 $cm^{-1}$. This complex was only observed at pH values above 6, where it co-existed with the second phosphate complex discussed above, and increased in concentration with increasing pH. We did not

find evidence for the formation of this particular phosphate species on hematite, which may indicate a difference in overall phosphate complexation on hematite and goethite at high pH values. Tejedor-Tejedor and Anderson [5] assigned this species as a monodentate mononuclear nonprotonated phosphate surface complex.

Persson et al. [6] used ATR-FTIR spectroscopy to characterize phosphate surface complexation on goethite and hematite as a function of pH, which was varied between 3.1 and 12.8. Similar to the results of Tejedor-Tejedor and Anderson [5] for phosphate sorption to goethite and our results for phosphate-reacted hematite, three different phosphate complexes were observed for the phosphate–goethite samples analyzed by Persson et al. [6], with the relative contributions of these complexes varying with pH. At low pH (3–4), a single phosphate complex with $\nu_3$ bands at 1178 and 1001 $cm^{-1}$ dominated the phosphate surface speciation. With increasing pH, a second complex with $\nu_3$ bands at 1122, 1049 and 939 $cm^{-1}$ became increasingly important, and this complex was the dominant phosphate surface species at pH 8–11. At pH 12.8, a third phosphate complex with IR bands at 1057 and 966 $cm^{-1}$ was the dominant surface species.

The pH trend observed in the phosphate–goethite data of Persson et al. [6] agrees with our results and those of Tejedor-Tejedor and Anderson [5], but there are differences in $\nu_3$ band positions of the various phosphate complexes. This is likely due to the ex-situ conditions used by Persson et al. [6] for IR data collection, which was done following drying and subsequent dilution of phosphate-reacted goethite in KBr. The water content in these samples is therefore low relative to the samples analyzed by Tejedor-Tejedor and Anderson [5] and in our studies, which were characterized in situ. This may affect the degree of hydrogen bonding between phosphate surface complexes and water molecules, which may explain the observed band shifts [6]. Sample drying and mixing in KBr may also lead to structural changes in surface complexes, as has been observed for sulfate complexation by hematite and goethite [10,12].

In addition to the spectral differences observed for the phosphate complexes formed on goethite, Persson et al. [6] also made different assignments as to the identity of the phosphate complexes than Tejedor-Tejedor and Anderson [5]. Whereas Tejedor-Tejedor and Anderson [5] favored monodentate binuclear (bridging) phosphate complexes at low and intermediate pH values and monodentate mononuclear complexes at high pH, Persson et al. [6] argued for the formation of strictly monodentate mononuclear phosphate surface complexes that are diprotonated, monoprotonated and nonprotonated at low, intermediate and high pH values, respectively.

In a second set of IR experiments, Persson et al. [6] studied phosphate complexation by hematite. In contrast to the goethite results, phosphate was found to predominantly form a surface precipitate on hematite, as evidenced by the predominance of broad IR features with superimposed finer band splitting, and a near-independence of phosphate IR features on pH. Precipitate formation was unexpected and ascribed to pretreatment of the hematite material, which was obtained by dry-grinding of single hematite crystals, possibly resulting in the presence of amorphous Fe(III)-(hydr)oxide surface layers on the hematite particles with sufficient Fe(III) solubility for formation of Fe(III)-phosphate precipitates to occur. In contrast, the hematite material used in our study was prepared from an aged aqueous suspension, as described in the material and methods section, and this likely explains the different results found in this study for phosphate complexation on hematite as compared to Persson et al. [6].

Arai and Sparks [7] characterized phosphate adsorption to ferrihydrite with in situ ATR-FTIR spectroscopy as a function of pH and phosphate surface coverage. Two different phosphate complexes were identified: at pH 4.0, a phosphate complex with broad $\nu_3$ bands centered at 1102, 1020 and 920 $cm^{-1}$ dominated the phosphate speciation at the ferrihydrite surface, whereas at pH $\geqslant$ 7.5, a complex with $\nu_3$ bands at 1088, 1021 and 952 $cm^{-1}$ was dominant; at pH 5 and 6, a mixture of these species was observed. No changes in phosphate speciation were observed as a function of the phosphate surface loading at pH 4 and 7.5. Comparison of IR spectra collected in $D_2O$ and $H_2O$ indicated that the complex formed at pH/pD = 7.5 was nonprotonated, since there was no difference in $\nu_3$ band positions between the $H_2O$ and $D_2O$ experiments. At pH/pD = 4, however, $\nu_3$ band shifting to lower wavenumbers for spectra recorded in $D_2O$ as compared to $H_2O$ indicated that the phosphate surface complexes formed under these conditions were protonated. Based on these experimental observations and using symmetry arguments, Arai and Sparks [7] assigned the surface complexes forming at pH $\geqslant$ 7.5 as nonprotonated monodentate binuclear (bridging) phosphate complexes, and the species forming at low pH 4 as protonated bridging complexes.

The results of Arai and Sparks [7] are consistent with our phosphate–hematite data, in that the mechanism of phosphate sorption is found to vary with pH, and protonated phosphate surface complexes are observed at low pH. The $\nu_3$ IR bands identified by Arai and Sparks [7] are somewhat different from those of the phosphate sorption complexes formed on hematite, which may reflect a difference in the speciation of phosphate adsorbed on ferrihydrite as compared to hematite. An important difference is that the phosphate complexes formed on ferrihydrite at high pH (7.5) are not protonated, whereas our results show that protonated phosphate surface complexes do exist at the hematite surface at these high pH values. The broad IR bands identified by Arai and Sparks [7] for the phosphate surface complexes formed on ferrihydrite may represent an assemblage of a series of overlapping (narrower) $\nu_3$ bands associated with a set of different phosphate surface complexes. The presence of multiple (slightly) different phosphate complexes at the ferrihydrite surface is not unlikely given the amorphous nature of this substrate, which likely leads to a larger variety in the characteristics of surface sites available for phosphate complexation than in the case of crystalline hematite. This could explain the broad IR bands observed by Arai and Sparks [7], and would also affect the peak maxima positions, as these reflect an intensity-average of the various overlapping $\nu_3$ bands involved.

Kwon and Kubicki [26] used quantum-mechanical calculations to simulate IR frequencies for a variety of different

phosphate inner-sphere complexes on Fe(III)-oxide phases. The results of these theoretical calculations were compared to the experimental data of the phosphate–goethite system reported by Persson et al. [6] and the phosphate–ferrihydrite data of Arai and Sparks [7]. Agreement between theoretical and experimental IR data reported by Persson et al. [6] for phosphate uptake by goethite lead to the assignment of diprotonated monodentate binuclear (bridging) phosphate complexes for the IR spectra observed at pH 4.2–5.7, either deprotonated bridging or monoprotonated monodentate mononuclear phosphate surface complexes forming at pH 7.9, and the formation of nonprotonated monodentate mononuclear phosphate complexes at pH 12.8. Based on the reaction energies calculated for the two phosphate species that may form at pH 7.9, Kwon and Kubicki [26] favored the option of monoprotonated monodentate mononuclear phosphate surface complexes forming at the goethite surface at this pH.

The experimental ATR-FTIR frequencies reported by Arai and Sparks [7] did not match the theoretical frequencies of any of the model complexes calculated by Kwon and Kubicki [26]. It was suggested that this may be due to the merging of individual $\nu_3$ bands associated with a single phosphate surface complex. Indeed, the peak maxima in the experimental spectrum obtained at pH 7.5 (assigned by Arai and Sparks [7] to a nonprotonated bridging surface complex) could successfully be reproduced by increasing the half-bandwidths of Gaussians centered at the theoretical $\nu_3$ peak positions of the nonprotonated bridging complex calculated by Kwon and Kubicki [26].

The applicability of the theoretical IR frequencies calculated by Kwon and Kubicki [26] to our phosphate–hematite data is uncertain. The match with the ex-situ IR data reported by Persson et al. [6] for phosphate complexation by goethite may reflect the relatively low degree of hydration used in the theoretical calculations, where four to six water molecules were included to account for the effect of solvation [26]. The difference in IR frequencies of phosphate–goethite surface complexes observed in the in situ studies by Tejedor-Tejedor and Anderson [5] as compared to the ex-situ results of Persson et al. [6] indicates that the degree of hydration may affect the positions of the IR frequencies of phosphate complexes, and this complicates the comparison of the theoretical calculations of Kwon and Kubicki [26] with our in situ IR data. Moreover, multiple phosphate sorption species are present at both the goethite and hematite surfaces simultaneously under most experimental conditions, which complicates the spectral isolation and structural assignment of individual phosphate species. Kwon and Kubicki [26] proposed the formation of diprotonated monodentate binuclear phosphate complexes on goethite at pH 4.2–5.7 based on the IR spectra collected by Persson et al. [6] in this pH range. However, two different phosphate species are thought to co-exist at the goethite surface under these pH conditions [5,6], as is the case for the results shown here for phosphate adsorption onto hematite.

Overall, phosphate sorption to Fe(III)-(hydr)oxide surfaces appears to vary with pH, and protonation of surface complexes is proposed in most studies, especially for the surface complexes forming at low pH. The studies referenced above differ mostly with respect to assignment of the coordination of the various phosphate complexes at the Fe(III) oxide surface and the proposed degree of protonation of the surface complexes. In the following section, our (tentative) structural assignments of the three phosphate surface complexes formed on hematite will be discussed.

### 4.2. Assignment of surface structures

We have identified the formation of three different phosphate complexes at the hematite–water interface. Spectra data fitting has indicated that two of these complexes have three active $\nu_3$ bands, whereas the third complex appears to have two $\nu_3$ bands. Based on symmetry arguments (illustrated in Fig. 1), this indicates that the first two phosphate complexes have $C_{2v}$ or lower ($C_1$) symmetry, whereas the third complex has $C_{3v}$ symmetry. The observed symmetry reduction of these complexes relative to the $T_d$ symmetry of the $PO_4^{3-}$ unit may result from phosphate coordination to both Fe and H atoms. The results of the $D_2O$ experiments showed that the two phosphate surface complexes with $C_{2v}$ or lower symmetry are associated with protons. However, comparison of the spectra of the variously protonated aqueous phosphate species shown in Fig. 1 to those of the two protonated phosphate complexes formed on hematite indicates substantial differences in $\nu_3$ band positions between these data sets. This indicates that the symmetry of these phosphate–hematite complexes is caused not by protonation only, but that phosphate atoms coordinate to iron atoms at the hematite surface as well, so that inner-sphere adsorption complexes are formed. Possible inner-sphere phosphate complexes consistent with the ATR-FTIR spectra are illustrated in Fig. 9.

Although not fully isolated, the phosphate complex with $C_{3v}$ symmetry has $\nu_3$ bands at similar positions as those of aqueous $HPO_4^{2-}$(aq), which is the dominant aqueous phosphate species in the pH range where this surface complex is observed. As noted in the materials and methods section, solutions were scanned following the sorption experiments to confirm that contributions from aqueous phosphate were negligible in the sorption spectra. Therefore, the $C_{3v}$ phosphate complex observed in our data is not due to contributions from aqueous $HPO_4^{2-}$, but represents an adsorbed phosphate species.

The similarity in band positions between $HPO_4^{2-}$(aq) and the $C_{3v}$ phosphate–hematite surface complex may indicate that this species is an outer-sphere or hydrogen-bonded surface complex held in the near-vicinity of the hematite surface by predominantly electrostatic forces. Since the $pH_{PZC}$ of hematite is approximately 8.2, and phosphate sorption shifts the $pH_{PZC}$ to lower pH values (e.g., [7,27,28]), the hematite surface was negatively charged at the experimental pH/pD values where the $C_{3v}$ species was observed (pH/pD = 8.5–9.0). This makes the formation of strictly outer-sphere sorption complexes unlikely, but it is possible that hydrogen-bonded phosphate complexes are formed under these conditions, as has been observed for borate and carbonate oxyanions at pH values above the point of zero charge of ferrihydrite and hematite, respectively [18,21]. However, rather than an outer-sphere or hydrogen-bonded surface

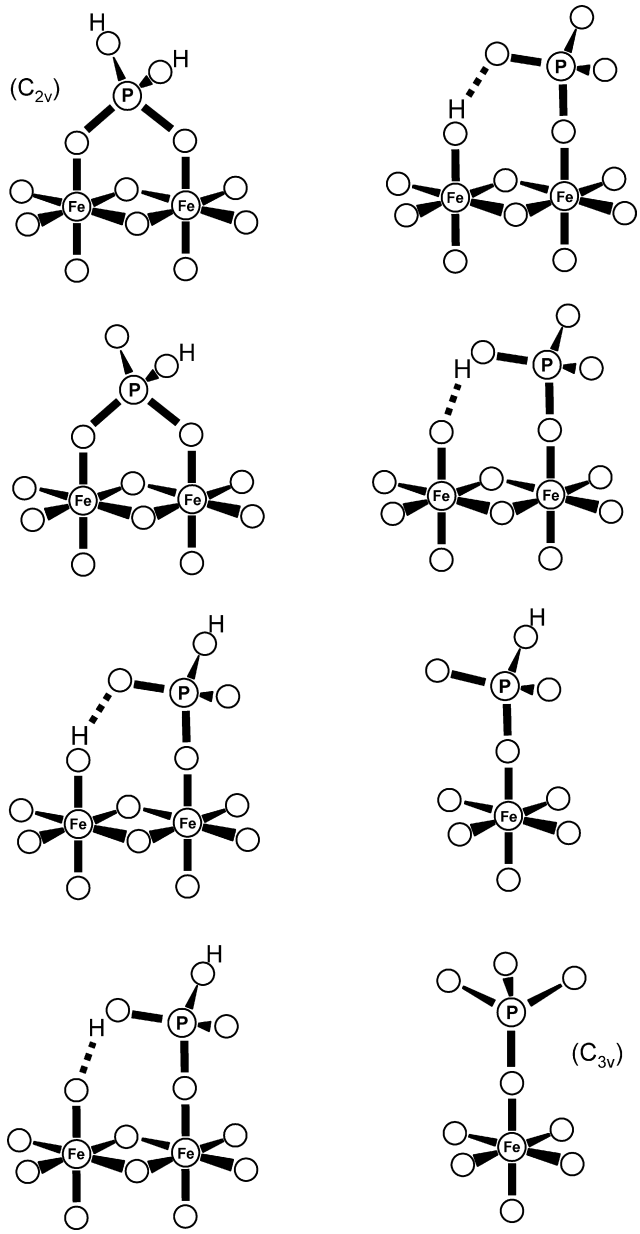


Fig. 9. Inner-sphere linkages of phosphate units to the hematite surface that are consistent with the ATR-FTIR data of the various phosphate–hematite surface complexes; the symmetry of these complexes is $C_1$ unless otherwise noted. Dashed lines represent hydrogen bonds.

complex, we favor the assignment of a monodentate nonprotonated inner-sphere complex for the $C_{3v}$ species. If a combination of inner- and outer-sphere complexation occurs, then it would be expected that the contribution from outer-sphere complexes would decrease at increased surface loadings, since the inner-sphere complexes would render the surface increasingly more negative at higher surface coverages, which would reduce the relative degree of outer-sphere complexation at higher coverages, as has been observed for sulfate adsorption to goethite [16,17]. The results from the high pH/pD sorption isotherms indicate, however, that the $C_{3v}$ complex in fact becomes increasingly more pronounced at higher surface loadings, which is inconsistent with this species being an electrostatically held surface complex. We therefore assign the phosphate complex with $C_{3v}$ symmetry, which forms at high pH values at relatively high surface loadings, as a nonprotonated monodentate phosphate surface complex (Fig. 9).

As noted earlier, the formation of monodentate nonprotonated phosphate surface complexes at high pH values has also been proposed by both Tejedor-Tejedor and Anderson [5] and Persson et al. [6] for phosphate complexation on goethite. The difference in IR spectral bands observed for these complexes (1025 and 1001 $cm^{-1}$ in Tejedor-Tejedor and Anderson [5], 1057 and 966 $cm^{-1}$ in Persson et al. [6], and approximately 1075 and 990 $cm^{-1}$ in our study) is likely a combination of the difficulty in separating the spectrum of this species from that of the second complex that forms at high pH with $\nu_3$ bands that are strongly overlapping with the monodentate species assigned here, differences in experimental procedures (in situ data collection in the case of Tejedor-Tejedor and Anderson [5] and in our study, versus ex-situ conditions used by Persson et al. [6]), and possibly due to differences in substrate surface properties (goethite versus hematite) that may affect the strength of Fe–$PO_4$ complexation.

Assignment of the two (protonated) phosphate–hematite complexes with $C_{2v}$ or $C_1$ symmetry is not straightforward, as reflected by the large number of possible configurations shown in Fig. 9 that are consistent with the ATR-FTIR spectra of these phosphate surface species. This illustrates the limited practical use of symmetry considerations in assigning structural configurations when a complete set of appropriate reference spectra is not available. The limitation of this approach arises from the fact that no distinction can be made between the H and Fe coordination, and that the number of $\nu_3$ bands is the same for complexes having $C_{2v}$ and lower symmetries, which makes their distinction problematic. Nevertheless, comparison of the aqueous phosphate species with those of the phosphate–hematite surface complexes provides some constraints on the structure assignment of the latter.

An important difference in the various phosphate surface complexes that are consistent with the IR spectra of the two species that form at the hematite surface in the pH range 3.5–8.5 is the degree of protonation: both monoprotonated and diprotonated surface species might account for the observed IR spectra of these species (Fig. 9). Formation of triprotonated phosphate surface species can be excluded, since such complexes would have $C_{3v}$ symmetry and therefore two $\nu_3$ bands, which is inconsistent with the IR data obtained. The IR spectra of the aqueous phosphate complexes in Fig. 1 show the presence of a band at 1240 $cm^{-1}$ for di- and triprotonated aqueous phosphate, assigned to the P–O–H bending mode $\delta$(POH), whereas this band is too weak to be discerned for monoprotonated phosphate (Fig. 1). Consequently, this band may be an indicator of the degree of phosphate protonation. The IR spectra of the two protonated phosphate–hematite surface complexes did not show any evidence of a $\delta$(POH) vibration band near 1240 $cm^{-1}$. This suggests that these phosphate species are monoprotonated.

A further difference between the various options of the phosphate–hematite surface complexes concerns the coordination of the phosphate complexes to the hematite surface: both

monodentate mononuclear and binuclear (protonated) complexes would be consistent with the IR data of these surface complexes. If both phosphate complexes are monoprotonated, as suggested by the absence of a discernible $\delta$(POH) vibration in their spectra, the difference in the IR spectra of these species reflects a coordination change from binuclear (bridging) to mononuclear linkage to the hematite surface. A monoprotonated bridging surface complex is expected to exhibit a $\nu$(P=O) vibration band at relatively high wavenumber due to a high degree of localization of the P=O double bond expected for this configuration. Based on this consideration, the surface complex favored at low pH and high surface coverage is assigned as a monodentate binuclear (monoprotonated) surface complex, as its IR spectrum has a band at $\sim$1120 $cm^{-1}$ that is consistent with $\nu$(P=O). By elimination, the complex forming at higher pH and low surface coverages is assigned as a monodentate mononuclear (monoprotonated) complex.

Hydrogen-bonding of phosphate anions to adjacent surface sites will lead to a phosphate surface coordination intermediate between monodentate mononuclear and binuclear linkage (Fig. 8). Although such a coordination will lower the symmetry of sorbed phosphate, the extent of the symmetry reduction is difficult to ascertain. If the hydrogen bond is relatively weak, the phosphate complex favored at low pH and high surface coverage is likely to be a "true" binuclear complex bridging two $FeO_6$ surface octahedra, whereas the monodentate mononuclear phosphate complex forming at higher pH and lower surface coverage may form a hydrogen bond to an adjacent surface site. If, on the other hand, strong hydrogen bonds are formed, the phosphate complex observed at higher pH and low surface coverage would be strictly mononuclear without hydrogen bonding to adjacent sites, whereas the phosphate complex favored at low pH and high surface coverage may be intermediate between a mononuclear and binuclear species as a result of hydrogen bond interaction with adjacent surface sites. Assessment of the phosphate coordination to the hematite surface by EXAFS spectroscopy would be useful to distinguish between these possibilities, as would be theoretical calculations on the effect of hydrogen bonding on phosphate IR bands. In either case, however, the main difference between these two monoprotonated surface species is that the "bridging" complex, favored under conditions of low pH and high surface coverage, interacts strongly with two hematite surface sites (either directly or via hydrogen bonding), whereas the mononuclear complex strongly interacts with only one surface site.

## 5. Conclusions

Phosphate adsorption on hematite was characterized as a function of pH (3.5–8.9) and phosphate concentration (5–500 μM) by in situ ATR-FTIR spectroscopy. The results indicated that under most conditions a mixture of different phosphate complexes exist at the hematite surface. Three different phosphate complexes were identified, and the relative importance of these complexes varied with pH and phosphate surface coverage. Experiments performed in $H_2O$ and $D_2O$ indicated the presence of two protonated phosphate surface complexes at low to intermediate pH/pD values (3.5–7.0). Comparison to spectra of variably protonated aqueous phosphate species suggest that these surface complexes are monoprotonated, although their exact protonation state could not be determined. The difference in IR spectra between these protonated species is tentatively interpreted to be the result of a difference in surface coordination, with one of the surface complexes bound in a monodentate binuclear (bridging) fashion to the hematite surface, and the second species coordinated as a monodentate mononuclear complex. Alternatively, the bridging complex may be a (protonated) monodentate mononuclear complex exhibiting strong hydrogen bonding to an adjacent surface site, whereas the second protonated surface species is a monodentate complex exhibiting no (or limited) hydrogen bonding. Formation of the bridging complex is favored at lower pH values and higher surface loadings in the 3.5–7.0 pH range. At the highest pH values studied here (pH 8.5–9.0), the bridging protonated phosphate complex is no longer observed, but a third complex, interpreted to be a nonprotonated monodentate mononuclear (inner-sphere) complex, is present in addition to the monodentate monoprotonated surface species. The importance of this nonprotonated monodentate complex increases relative to the protonated monodentate species as the surface coverage is increased at these high pH values.

## Acknowledgments

We thank Dr. Yuji Arai (USGS, Menlo Park) for providing the hematite sorbent used in the experiments and for reviewing an early draft of this manuscript. The comments of two anonymous reviewers further improved this paper.

## References

[1] R.J. Atkinson, R.L. Parfitt, R.S.C. Smart, J. Chem. Soc. Faraday Trans. 1 70 (1974) 1472.
[2] R.L. Parfitt, J.D. Russell, V.C. Farmer, J. Chem. Soc. Faraday Trans. 1 72 (1976) 1082.
[3] R.L. Parfitt, R.J. Atkinson, Nature 264 (1976) 740.
[4] R.L. Parfitt, R.J. Atkinson, R.S.C. Smart, Soil Sci. Soc. Am. Proc. 39 (1975) 837.
[5] M.I. Tejedor-Tejedor, M.A. Anderson, Langmuir 6 (1990) 602.
[6] P. Persson, N. Nielsson, S. Sjöberg, J. Colloid Interface Sci. 177 (1996) 263.
[7] Y. Arai, D.L. Sparks, J. Colloid Interface Sci. 241 (2001) 317.
[8] K. Nakamoto, Infrared and Raman Spectra of Inorganic and Coordination Compounds, Wiley, New York, 1997.
[9] G. Lefèvre, Adv. Colloid Interface Sci. 107 (2004) 109.
[10] S.J. Hug, B. Sulzberger, Langmuir 10 (1994) 3587.
[11] S.J. Hug, J. Colloid Interface Sci. 188 (1997) 415.
[12] D. Peak, R.G. Ford, D.L. Sparks, J. Colloid Interface Sci. 218 (1999) 289.
[13] H. Wijnja, C.P. Schulthess, Spectrochim. Acta A 55 (1999) 861.
[14] H. Wijnja, C.P. Schulthess, J. Colloid Interface Sci. 229 (2000) 286.
[15] H. Wijnja, C.P. Schulthess, Soil Sci. Soc. Am. J. 65 (2001) 324.
[16] E.J. Elzinga, D. Peak, D.L. Sparks, Geochim. Cosmochim. Acta 65 (2001) 2219.
[17] D. Peak, E.J. Elzinga, D.L. Sparks, in: H.M. Selim, D.L. Sparks (Eds.), Heavy Metals Release in Soils, Lewis Publishers, Boca Raton, FL, 2001.
[18] D. Peak, G.W. Luther, D.L. Sparks, Geochim. Cosmochim. Acta 67 (2003) 2551.

[19] M. Villalobos, J.O. Leckie, J. Colloid Interface Sci. 235 (2001) 15.
[20] J.R. Bargar, R. Reitmeyer, J.A. Davis, Environ. Sci. Technol. 33 (1999) 2481.
[21] J.R. Bargar, J.D. Kubicki, R. Reitmeyer, J.A. Davis, Geochim. Cosmochim. Acta 69 (2005) 1527.
[22] P.A. Connor, A.J. McQuillan, Langmuir 15 (1999) 2916.
[23] K.W. Paul, M.J. Borda, J.D. Kubicki, D.L. Sparks, Langmuir 21 (2005) 11071.
[24] U. Schwertmann, R.M. Cornell, Iron Oxides in the Laboratory: Preparation and Characterization, VCH Publishers, Weinheim, 1991.
[25] C. Luengo, M. Brigante, J. Antelo, M. Avena, J. Colloid Interface Sci. 300 (2006) 511.
[26] K.D. Kwon, J.D. Kubicki, Langmuir 20 (2004) 9249.
[27] J. Ren, A.I. Packman, Environ. Sci. Technol. 39 (2005) 6387.
[28] J. Antelo, M. Avena, S. Fiol, R. Lopez, F. Arce, J. Colloid Interface Sci. 285 (2005) 476.